Available online at www.sciencedirect.com
ScienceDirect
Polymer 49 (2008) 1365–1375
polymer
www.elsevier.com/locate/polymer

Crystallization kinetics of some new olefinic block copolymers

D.U. Khariwala [a], A. Taha [b], S.P. Chum [b], A. Hiltner [a,*], E. Baer [a]

[a] Department of Macromolecular Science and Center for Applied Polymer Research, Case Western Reserve University, Cleveland, OH 44106-7202, United States
[b] Performance Plastics and Chemicals R&D, The Dow Chemical Company, Freeport, TX 77541, United States

Received 16 October 2007; received in revised form 20 December 2007; accepted 23 December 2007
Available online 12 January 2008

Abstract

Blocky ethylene–octene copolymers synthesized by chain-shuttling polymerization differ from statistical copolymers in their rapid rate of crystallization and in the formation of space-filling spherulites even when the crystallinity is as low as 7%. The bulk crystallization rate, measured with DSC, was rapid even in copolymers with a relatively large fraction of non-crystallizable soft block and only slowed somewhat as the amount of crystallizable hard block decreased from 100 to 18 wt%. As measured with the polarized optical microscope, the linear spherulite growth rate exhibited the same dependence on soft block content as the bulk crystallization rate. The fold surface energy was extracted from an analysis of the growth rate according to the Lauritzen–Hoffman theory. A gradual increase in the fold surface energy with soft block content reflected some increasing disorder of the fold surface. In contrast, even a small amount of statistically distributed comonomer was very effective in disrupting the fold surface regularity as demonstrated by the high fold surface energy.

Keywords: Olefin block copolymer; Crystallization kinetics; Spherulite

1. Introduction

Recent developments in polyolefin synthesis by The Dow Chemical Company enable synthesis of olefinic block copolymers (OBCs) in a direct way [1]. The block copolymers synthesized by chain-shuttling technology consist of crystallizable ethylene–octene blocks with very low comonomer content and high melting temperature, alternating with amorphous ethylene–octene blocks with high comonomer content and low glass transition temperature. The new blocky copolymers differ from anionically polymerized and hydrogenated olefin block copolymers in having a statistical multiblock architecture with a distribution in block lengths and a distribution in the number of blocks per chain. Nevertheless, the crystallizable blocks are long enough to form well-organized lamellar crystals with the orthorhombic unit cell and high melting temperature [2]. The hard blocks crystallize as space-filling spherulites even in blocky copolymers with only 7% crystallinity.

The impact of the blocky architecture is apparent when the crystallization habit is compared with that of statistical ethylene–octene copolymers [3]. In contrast to statistical copolymers, the blocky architecture imparts a substantially higher crystallization temperature and a higher melting temperature while maintaining a lower glass transition temperature. The differences between blocky and statistical copolymers become progressively more apparent as the comonomer content increases. In contrast to the small fringed micellar crystals of statistical copolymers, the blocky copolymers crystallize as lamellar spherulites. Further understanding of the crystallization behavior of the blocky copolymers is needed.

Like the anionically polymerized block copolymers, the OBCs are subject to the constraints imposed by covalently linked crystallizable and non-crystallizable blocks. The relationship between microphase separation and chain-folded crystallization has been explored in some depth over the past 25 years with semicrystalline block copolymers having

* Corresponding author. Department of Macromolecular Science and Center for Applied Polymer Research, Case Western Reserve University, Kent Hale Smith Building, Room 423, 10900 Euclid Avenue, Cleveland, OH 44106-7202, United States.
E-mail address: ahiltner@case.edu (A. Hiltner).

0032-3861/$ - see front matter © 2008 Elsevier Ltd. All rights reserved.
doi:10.1016/j.polymer.2007.12.046

well-defined block lengths and narrow molecular weight distributions. In almost all cases, the crystallizable block was hydrogenated butadiene, which, in chemical structure, closely resembled the low comonomer hard block of OBCs. These previous studies provide a valuable reference for studying the crystallization behavior of statistical blocky copolymers.

The simple phase diagram of olefin block copolymers is described by the relative amount of each block and the quantity χN, where χ is the Flory–Huggins interaction parameter and N is the total degree of polymerization. Based on the quantity χN, it is convenient to describe block copolymers as miscible, weakly segregated close to the order–disorder transition, or strongly segregated [4]. If one of the blocks is crystallizable, the melt regime significantly impacts its crystallization habit.

For the homogeneous melt, a layered morphology of alternating crystalline lamellae and amorphous blocks is established at the crystallization temperature as soon as one of the blocks crystallizes [5,6]. The lamellar morphology shows a high degree of long range order with spherulitic organization. Spherulitic textures have been reported even when the crystallinity is very low [7]. Crystallization kinetics from a homogeneous melt conforms to the Avrami theory with $n = 3$ and heterogeneous nucleation [8]. The effect of the non-crystallizable block is to retard crystallization to some extent compared to the corresponding homopolymer [5].

The well-developed spherulitic morphology of OBCs is consistent with crystallization from a homogeneous melt. Although the hard and soft blocks differ considerably in the comonomer content, the blocks are short enough to be miscible in the melt. The direct and economical synthesis of the OBCs in substantial quantity makes it possible to employ conventional methods for studying polymer crystallization kinetics. This paper describes the bulk crystallization kinetics and spherulite growth rate of statistical blocky copolymers that vary in the fraction of hard block. The data are analyzed, respectively, according to the Avrami theory and the Lauritzen–Hoffman theory.

2. Materials and methods

The blocky ethylene–octene copolymers (OBCs) were supplied as pellets by The Dow Chemical Company, together with information on block content, molecular weight and molecular weight distribution, as reported previously [2]. Results from the statistical analysis of the chain-shuttling phenomenon were also provided by Dow. Homogeneous ethylene–octene copolymers (EOs) with essentially the same comonomer content as the hard block (0.5 mol% octene) and as the soft block (18.9 mol% octene) were used as controls and are designated as HS and SS. The weight percent hard block in the blocky copolymers was calculated from the weight percent total octene [2]. The blocky copolymers are designated as $(EO0.5)_x$-b-$(EO18.9)_{100-x}$ where EO0.5 is the hard block, EO18.9 is the soft block, and x is the hard block content as weight percent. For convenience, a shorter sample code, Hx is used hereafter. The local comonomer distribution within the hard and soft blocks was statistical and homogeneous.

Two additional resins were included in the study. One was a reactor blend of hard blocks and soft blocks that was synthesized with the same catalyst combination as the OBCs but without the chain-shuttling agent [1]. The reactor blend had 26 wt% HS and it is designated as H26RB. A statistical ethylene–octene copolymer containing 2.8 mol% octene (EO2.8) was also used for comparison. The synthesis and properties were described previously [9,10].

Films of 0.5 mm thickness were compression molded from the pellets. The pellets were sandwiched between Mylar® sheets and pre-heated at 190 °C for 5 min under minimal pressure, cycled from 0 to 10 MPa pressure for 1 min to remove air bubbles, held at 10 MPa for 4 min and cooled to ambient temperature at approximately 15 °C min^{-1} in the press. The compression-molded films were subsequently stored at ambient temperature for 7–12 days before performing further experiments.

Density was measured according to ASTM D1505-85 using small pieces cut from the compression-molded films. An isopropanol–water gradient column with a density range of 0.8–1.0 g cm^{-3} was used. The reported density is the average of at least 3 specimens and has an error of less than 0.0005 g cm^{-3}. It was noted that crystallinity calculated from the two-phase density model, using the established crystalline and amorphous phase densities for polyethylene [11], correlated with the DSC crystallinity for all the ethylene–octene copolymers as well as for the reactor blend.

Specimens weighing 5–10 mg were cut from compression-molded films for thermal analysis. Thermal analysis was carried out in a Perkin–Elmer DSC7 calibrated with indium and tin standards. Heating and cooling thermograms were taken between −50 and 190 °C with a heating/cooling rate of 10 °C min^{-1}. For isothermal bulk crystallization, the number of extra lids in the reference aluminum pan was adjusted to balance the heat capacity and achieve the best baseline. Specimens were melted at 250 °C for 5 min and rapidly cooled at 100 °C min^{-1} to the crystallization temperature T_x. A new specimen was used for each isothermal test. The determination of time $t = 0$ for the kinetic analysis merits some discussion. The assumption that no crystallization occurs before the specimen reaches the crystallization temperature is usually acceptable because the onset of crystallization usually requires an induction period. This assumption becomes less tenable as the isothermal crystallization rate increases. To minimize the time required to achieve a stable instrumental baseline, the number of lids in the reference pan was adjusted [12]. It was usually possible to reach a stable isothermal baseline in 0.4 min. The time t for the kinetic analysis was taken as the elapsed time minus 0.4 min.

Specimens for small angle X-ray scattering (SAXS) were isothermally crystallized at the target temperature and rapidly quenched to ambient temperature. The SAXS was carried out with a Rigaku MICROMAX-002–25W Microfocus Bede/Osmis XG system which is based on microfocusing Cu X-ray source coupled with a Confocal Max-FluxTM (CMF) optics. It provides a monochromatic focused hard X-ray beam by combining a ‘‘side-by-side’’ approach to the Kirkpatrick–Baez

scheme with high performance multilayers. A two-dimensional MULTI-WIRE detector was attached. Lorentz correction of the SAXS results was done by multiplying the intensity (counts per second) by q^2 ($q = 4\pi \sin\theta/\lambda$, where λ is the X-ray wavelength of 1.541 Å).

Isothermal spherulitic growth rate was determined by measuring the spherulite radius as a function of time at a given temperature in an Olympus BH-2 optical microscope (OM) equipped with a Mettler FP2 hotstage. Specimens were prepared by sandwiching 1 mg of sample between glass slides and heating at 200 °C for 5 min on a hot plate. The specimen was quickly transferred to the hotstage in the OM. To avoid degradation, specimens were crystallized under nitrogen and a different specimen was used for each crystallization temperature. During crystallization, digital micrographs were taken at regular time intervals. A λ/4-plate was used to enhance the contrast between birefringent spherulites and the isotropic melt. Image analysis software Image-J was used to measure the spherulite radius.

3. Results and discussion

3.1. Thermal properties and bulk crystallization kinetics

The hard and soft blocks of the blocky copolymers differed considerably in comonomer content. However, they were short enough to be miscible in the melt. This was confirmed by the homogeneous texture in AFM images of the quenched melt. On the other hand, the blocks were long enough that the hard blocks could form chain-folded lamellar crystals [2]. During crystallization, organization of the hard block lamellae into space-filling spherulites forced segregation of the non-crystallizable soft blocks into the interlamellar regions. Typically the impinged, isothermally crystallized spherulites showed straight boundaries, which indicated heterogeneous nucleation with nuclei of the same activity. Time-dependent nucleation would have resulted in curved boundaries between impinged spherulites [13]. Furthermore, similarity in spherulite size regardless of soft block content or crystallization temperature suggested almost constant nucleation density for these blocky copolymers. The primary effect of increasing soft block content was to decrease the packing density of the lamellae due to accommodation of a larger fraction of amorphous material in the interlamellar regions.

Thermograms of HS, SS and the blocky copolymers showed sharp melting and crystallization peaks [2]. The homogeneous copolymer HS, which had the same comonomer content as the hard block, showed a peak melting temperature T_m at 126 °C. The peak melting temperature of the crystalline hard blocks in the blocky copolymers shifted only slightly as the amount of hard block decreased, Table 1. The primary effect of composition was a proportional change in the transition enthalpy. Small changes in the crystallization temperature T_c paralleled the decrease in melting temperature, with the result that the undercooling ($T_m - T_c$) was about 20 °C for HS and for all the blocky copolymers except H18.

Isothermal crystallization was carried out at various temperatures in the vicinity of T_c. The DSC curves for all polymers showed a single peak as is typical for isothermal polymer crystallization. The relative crystallinity x_t is defined as the ratio of the crystallinity at time t, X_t, to the crystallinity at the time of completion, X_∞, and is given as

$$x_t = \frac{X_t}{X_\infty} = \frac{\int_0^t \left(\frac{dH}{dt}\right) dt}{\int_0^\infty \left(\frac{dH}{dt}\right) dt} = \frac{\Delta H_t}{\Delta H_\infty} \quad (1)$$

where dH/dt is the rate of heat evolution, ΔH_t is the total heat evolved at time t, and ΔH_∞ is the total heat evolved at completion. For all the copolymers, ΔH_∞ decreased with increasing crystallization temperature [14]. Plots of the relative crystallinity as a function of time showed the sigmoidal shape typical of isothermal polymer crystallization. The halftime of crystallization $t_{1/2}$ was defined as the time required to reach $x_t = 0.5$. Typically, $t_{1/2}$ represented the overall crystallization rate and was governed by the rates of nucleation and growth.

The combined effects of nucleation and growth produce a maximum in the crystallization rate at a temperature between the melting point and the glass transition temperature, which gives rise to the so-called bell curve of isothermal crystallization [15]. For all the polymers in this study, increasing $t_{1/2}$ with crystallization temperature indicated that the

Table 1
Physical properties of copolymers

Material	Total octene (mol%)	Hard block content (wt%)	Density (g/cm^3)	T_m (°C)	ΔH_m (J/g)	X_c (DSC) (wt%)	T_c (°C)	$T_m - T_c$ (°C)	T_β (log E'') (°C)	σ_e (erg cm^{-2})
HS	0.5	100	0.9349	126	170	59	109	17	–	111
H82	2.7	82	0.9202	124	137	47	104	20	−32	126
H57	6.6	57	0.9022	121	89	31	100	21	−44	131
H40	9.5	40	0.8929	119	79	27	98	21	−49	139
H27	12.2	27	0.8795	118	49	17	94	24	−51	143
H18	14.2	18	0.8649	114	15	7	74	41	−52	141
SS	18.9		0.8582	–	–	–	–	–	−52	–
EO2.8	2.8		0.9184	113	130	45	96	17	−27	204
H26RB	11.4		0.8753	125	41	14	104	21	−52	112

experiments were carried out on the high temperature side of the bell curve. The effect of soft block content on the temperature dependence of $t_{1/2}$ is shown in Fig. 1. With the exception of H18, the block copolymers showed about the same temperature dependence with a shift along the temperature axis that paralleled the change in T_m. However, as a consequence of the relatively strong temperature dependence of $t_{1/2}$, an increase in the soft block content resulted in a substantial decrease in the crystallization rate at any given temperature. The exception was H18, which exhibited a much weaker temperature dependence of crystallization rate. The weak temperature dependence, compared to the other blocky copolymers, would have originated from differences in nucleation and/or growth rate.

The Avrami analysis is generally thought to have limited value for polymer crystallization [16], nevertheless it can be useful for characterizing the bulk crystallization behavior. The classic Avrami equation is given as [15]

$$1 - X_t = \exp(-kt^n) \tag{2}$$

where k is the crystallization rate constant and n is the Avrami exponent describing the crystal growth geometry and nucleation mechanism. The data are plotted according to

$$\ln[-\ln(1 - X_t)] = n \ln t + \ln k \tag{3}$$

to obtain the Avrami parameters n and k. Typical results for H82 and H18 in Fig. 2 show that the Avrami plots were close to linear with deviation only at longer times. For consistency, n and k were always calculated from the linear portion of primary crystallization between $x_t = 0.05$ and $x_t = 0.80$.

The exponent n was always close to 3.0 [14], corresponding to three-dimensional spherulitic growth with athermal nucleation [17]. The rate constant k incorporated the growth rate and nucleation density. For the blocky copolymers, similarity in spherulite size regardless of soft block content or crystallization temperature suggested constant nucleation density. Thus, differences in k reflected primarily differences in growth rate. For each of the copolymers, k decreased with increasing temperature and, at a given temperature, the rate constant decreased with soft block content.

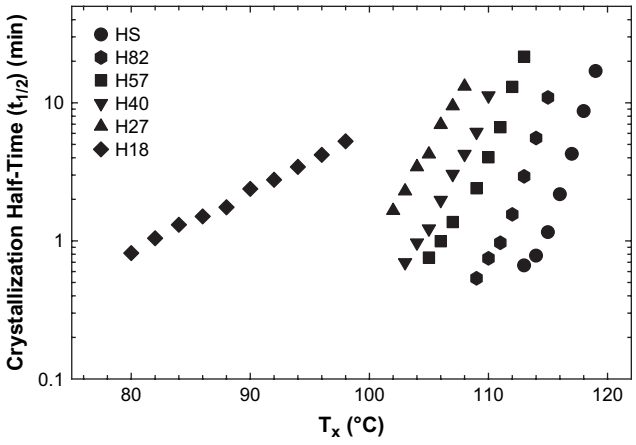

Fig. 1. Effect of soft block content on the temperature dependence of $t_{1/2}$.

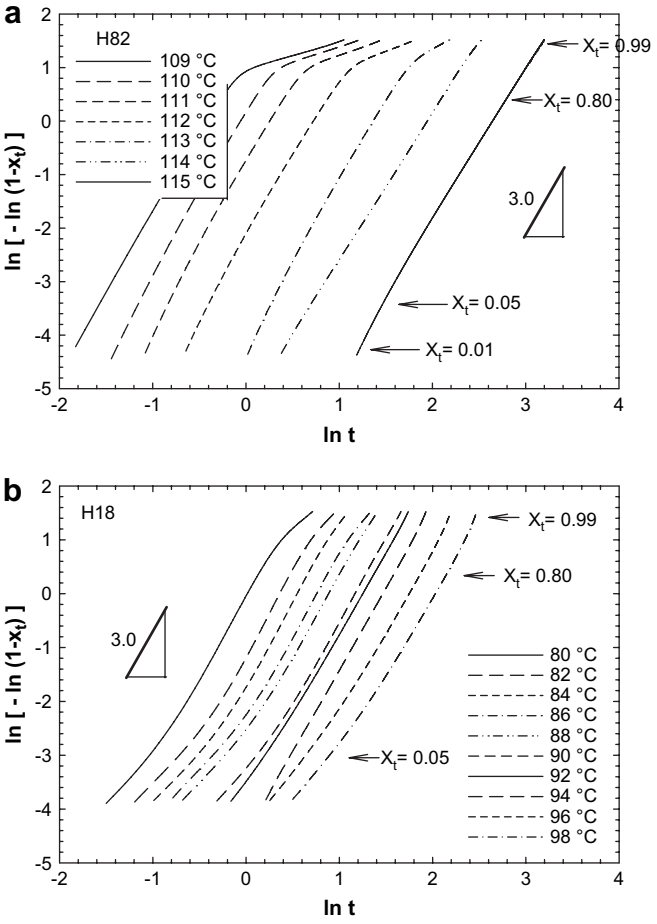

Fig. 2. Avrami plots for isothermal crystallization: (a) H82 and (b) H18.

3.2. Spherulite growth rate

The blocky copolymers crystallized as spherulites with negative birefringence and sharp boundaries. The spherulitic morphology varied only slightly with temperature. The average spherulite size increased slightly at higher temperatures, indicating that the nucleation density decreased slightly. The band spacing, which was observed in spherulites of the higher crystallinity copolymers HS, H82, H57 and H40, increased with temperature. A similar increase in band spacing has been observed in HDPE [18].

Isothermal spherulitic growth of H82 and H18, the blocky copolymers with the highest and lowest hard block content, is shown in Fig. 3. All the blocky copolymers exhibited a linear increase in the spherulite radius with time until impingement, even H18 which had only 7% crystallinity. The slope of the plots provided the linear growth rate G.

The temperature dependence of the growth rate for the various copolymers is shown in Fig. 4. As expected G decreased as the crystallization temperature approached the melting temperature. The slightly lower growth rate of HS, compared to that reported for HDPE spherulites [19,20], was consistent

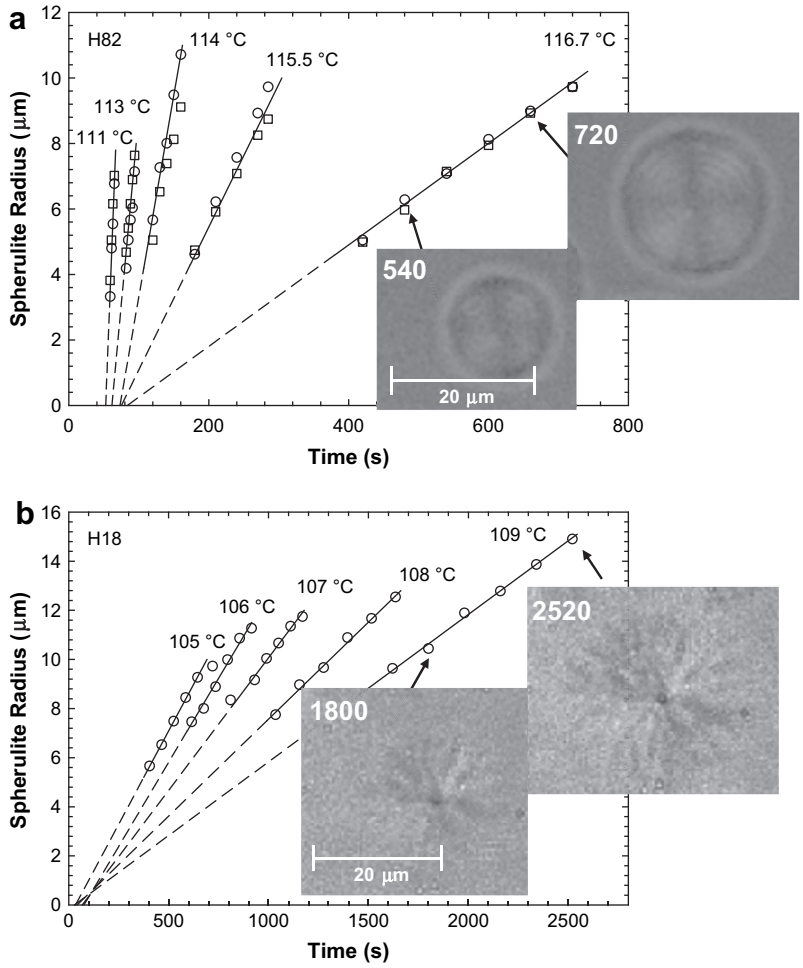

Fig. 3. Spherulite growth as a function of time at various temperatures: (a) H82 and (b) H18. Different symbols for a given temperature represent growth of different spherulites. The solid line is the best fit through the data points; the slope determines the growth rate. The dashed line is the extrapolation to $t = 0$ to determine the induction time.

with the observed decrease in growth rate with increasing comonomer content of ethylene copolymers [19]. Increasing the soft block content retarded crystallization of HS in terms of the spherulite growth rate due to rejection of the non-crystallizable soft block from the growth front. In addition to a reduced growth rate, Fig. 4 showed that the temperature dependence of the growth rate weakened with increasing soft block content. However, the temperature dependence of H18 spherulite growth rate was not dramatically different from that of the other copolymers, in contrast to the bulk crystallization rate (Fig. 1). Hence the weak temperature dependence of H18 bulk crystallization was attributed to a nucleation effect.

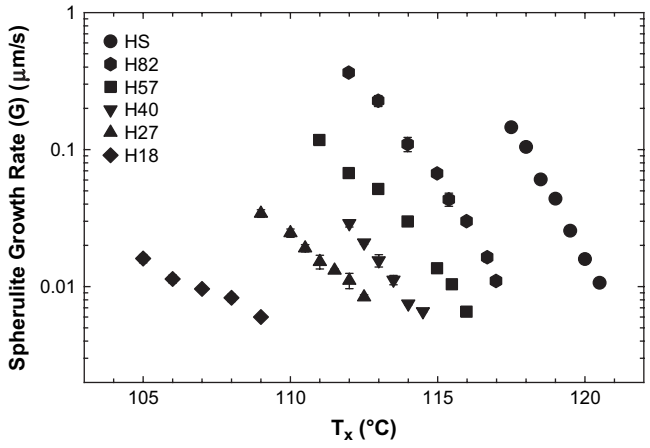

Fig. 4. Effect of soft block content on the temperature dependence of the spherulite growth rate.

In all cases, there was a certain induction time t_i before spherulites were detected in the OM. The induction time was deduced by extrapolating the linear growth to zero (see Fig. 3). The induction time increased with crystallization temperature [21], reflecting the longer time required for formation of the critical nucleus [22]. At a particular temperature, copolymers with higher soft block content also required a longer time to form the critical nucleus.

3.3. Effect of chain architecture on crystallization kinetics

Certain properties of ethylene–octene copolymers are not strongly affected by the comonomer distribution. For example,

crystallinity depends primarily on the comonomer content, not on whether the distribution is blocky or statistical [2]. Accordingly, bulk properties that depend on crystallinity, such as modulus and yield stress at ambient temperature, and even the stress–strain behavior, depend on comonomer content in the same way for statistical or blocky copolymers. However, substantially higher melting and crystallization temperatures and well-ordered spherulitic morphologies vividly differentiate blocky from statistical copolymers. This impacts the melt processing of the copolymers and their performance at higher temperatures. Blocky copolymers with even the highest comonomer content exhibit a spherulitic crystallization habit [2]. In contrast, only statistical copolymers with relatively low comonomer content crystallize as space-filling spherulites [3,10]. Thus, the impact of comonomer distribution on crystallization kinetics can best be demonstrated with copolymers having about 3 mol% (10 wt%) comonomer.

The comparison was made between crystallization of the statistical copolymer EO2.8 ($\rho = 0.9184$ g cm^{-3}) and crystallization of H82 ($\rho = 0.9202$ g cm^{-3}). A crystallization temperature of 96 °C in the cooling thermogram of EO2.8 compared to 104 °C for the blocky copolymer (H82) indicated that the statistical copolymer crystallized substantially more slowly than the blocky copolymer. In addition to the significant difference in peak crystallization temperature, the crystallization exotherm of the statistical copolymer as well as the subsequent melting endotherm were substantially broader, which reflected the broad crystal size distribution resulting from the statistical distribution of crystallizable sequence lengths.

The halftimes for bulk isothermal crystallization of EO2.8 and H82 are compared in Fig. 5a. The results for EO2.8 were shifted about 10 °C lower than the results for H82. In terms of bulk crystallization rate, EO2.8 most closely resembled H27, which had almost 11 mol% comonomer. The Avrami plots for EO2.8 had a slope close to 3.0, consistent with spherulitic growth and athermal nucleation. However, the pronounced curvature of the plots, in contrast to the linear Avrami plots of the blocky copolymers, reflected the broad distribution of crystallizable sequence lengths in the statistical copolymer.

The spherulites of EO2.8 resembled those of H82 in size and in their negative birefringence. However, the boundaries were not as sharp, the negative birefringence was not as well developed, and there was no banding. The spherulite growth was linear, however, the linear growth rate was considerably slower than the growth rate of H82 spherulites, Fig. 5b. The shift by about 10 °C lower in temperature was the same as observed in the bulk crystallization rate.

3.4. Crystallization of a hard and soft block blend

The effect of the covalent linkage between hard and soft blocks was examined by comparing crystallization of H27 ($\rho = 0.8795$ g cm^{-3}) with crystallization of the reaction product obtained without the shuttling agent. The particular catalyst system produced a "reactor blend" (H26RB) ($\rho =$ 0.8753 g/cm^3) with a bimodal molecular weight distribution

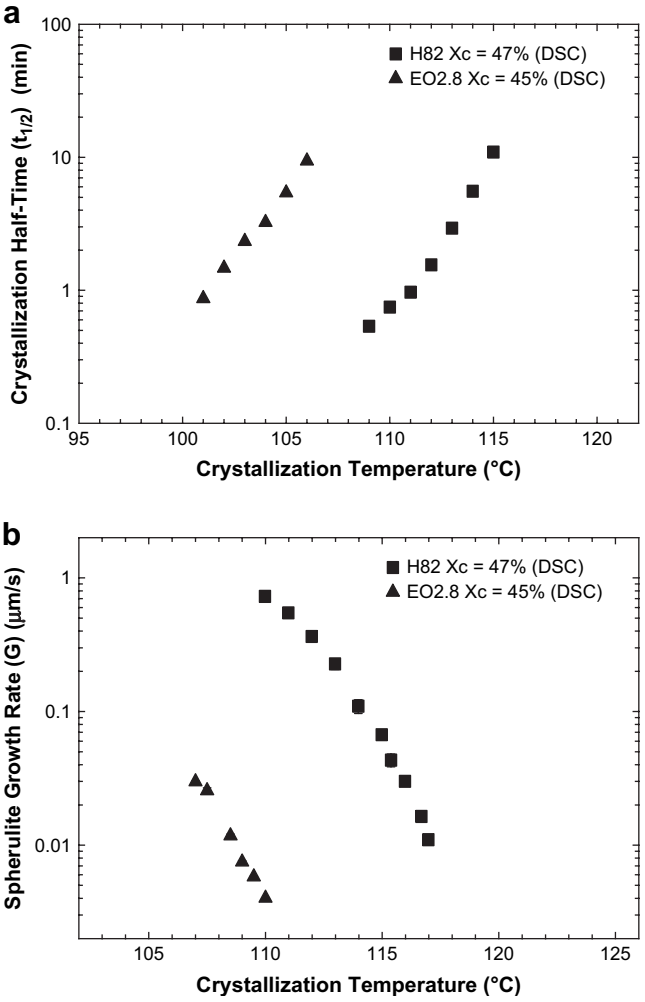

Fig. 5. (a) Comparison of the bulk crystallization kinetics of EO2.8 and H82 and (b) comparison of spherulite growth rate of EO2.8 and H82.

[1], which consisted of very low molecular weight hard block polymer ($M_w = 10$ kg/mol) and high molecular weight soft block polymer ($M_w = 200$ kg/mol). The blend with 26 wt% hard block was homogeneous in the melt. Presumably the miscibility resulted from the extremely low molecular weight of the hard block.

The bulk crystallization halftimes in Fig. 6a indicated that H26RB crystallized more rapidly than H27 and almost as rapidly as HS. Faster crystallization of H26RB compared to H27 revealed the inhibiting effect of the covalent linkages between crystallizable hard blocks and non-crystallizable soft blocks. On the other hand, the presence of soft block in the blend inhibited diffusion of hard block to the crystallization growth front, which accounted for the slightly lower bulk crystallization rate of H26RB compared to that of HS. The Avrami exponents were consistently about 2.0, Fig. 6b. The Avrami analysis assumes a constant growth rate and deviations are expected if the growth rate is time dependent [16,22], which is often the case in crystallization from a miscible blend [23].

The spherulites of H26RB in Fig. 7a had the open-armed or sheath-like appearance typical of spherulites grown from a miscible polymer blend [24]. The open-armed structure

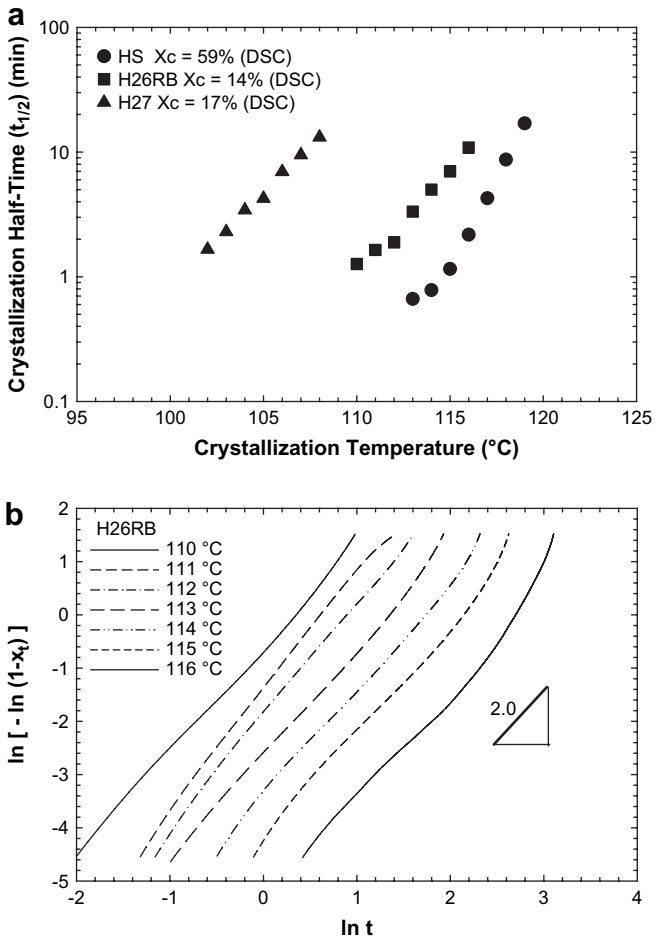

Fig. 6. Bulk crystallization kinetics of the reactor blend H26RB: (a) comparison of the crystallization halftimes of HS, H26RB and H27 and (b) Avrami plots for isothermal crystallization of H26RB.

formed when the excluded soft blocks segregated into the intra-spherulitic regions between growing lamellar arms. At lower crystallization temperatures the spherulite growth was linear with time and the spherulites were space filling. At higher crystallization temperatures, where the growth was slower and the nucleation density was somewhat lower, the initial linear growth gradually became parabolic at longer times, as was expected when the non-crystallizable polymer was excluded from the spherulite [25,26]. In this case, the crystallization rate was slow enough for rejected soft block to diffuse to the inter-spherulitic melt. The steadily increasing concentration of soft block in the uncrystallized melt inhibited diffusion of hard block to the growth front and thereby reduced the growth rate [27]. At 120 °C, spherulites had not impinged even after very long times due to segregation of soft block in the inter-spherulitic regions. In the blocky copolymers, covalent bonds between hard and soft blocks prevented this type of phase segregation during crystallization. Rather, the soft blocks were confined to the interlamellar regions, which allowed the formation of well-organized, space-filling spherulites even in blocky copolymers with very high soft block content.

The spherulite growth rates for the reactor blend were obtained from the linear portions of the growth plots, Fig. 7b. Without the constraints imposed by covalent bonds to the soft blocks, H26RB spherulites grew substantially faster than those of H27, the blocky copolymer with similar hard block content. Indeed, the presence of soft block polymer appeared to have essentially no effect, and the initial growth rates of H26RB and HS were about the same. However, the lamellae were not as densely packed as those of HS and moreover the growth rate slowed with time and became parabolic. These effects resulted in slower bulk crystallization of H26RB compared to HS. The unconventional spherulite growth habit of H26RB was also responsible for the deviation in the Avrami exponent from a value of 3.

3.5. Analysis of spherulite growth rate

The product of the chain-shuttling process is a multiblock copolymer with a distribution of block lengths and a distribution in the number of blocks per chain. A statistical analysis of the chain-shuttling phenomenon reveals the copolymers to have a most probable distribution of block lengths and number of blocks per chain. Preliminary model calculations of the polymer used in this study predict that the bulk of the polymer has between 2 and 10 blocks per chain. The molecular weight of the average hard block of an H82 chain with 6 blocks (3 hard blocks) would be 28 kg/mol or ~1900 C atoms in the backbone. The corresponding values would be 21 kg/mol or ~1400 C atoms for H57, 15 kg/mol or ~1000 C atoms for H40, 11 kg/mol or ~800 C atoms for H27 and 7 kg/mol or ~500 C atoms for H18. The average length of the hard block for all the copolymers is substantially longer than 80 C atoms required for a 10 nm lamellar stem, and hence the hard blocks are long enough to crystallize as chain-folded crystals.

The Hoffman–Lauritzen theory for spherulite growth considers two processes occurring at the growth front. The first process is the deposition of a secondary nucleus on the growth face and the second process is the subsequent growth along the face at the niches formed by the secondary nucleus [28]. The general form of the secondary nucleation theory is

$$G = G_0 \exp\left(-\frac{U^*}{R(T_x - T_\infty)}\right)\exp\left(-\frac{K_g}{T_x \Delta T}\right) \tag{4}$$

Experimental data are usually analyzed with Eq. (4) in the logarithmic form

$$\log G + \frac{U^*}{2.303R(T_x - T_\infty)} = \frac{(-K_g/2.303)}{T_x \Delta T} + \log G_0 \tag{5}$$

by plotting $\log G + U^*/2.303R(T_x - T_\infty)$ versus $1/T_x\Delta T$. Here G is the linear growth rate, U^* is the activation energy for transport of the blocks to the crystallization site, R is the gas constant, T_x is the crystallization temperature, T_∞ is the temperature at which all motions associated with viscous flow cease and is taken as T_g −20 °C. In this case, T_g was taken as the temperature of the DMTA β-relaxation, Table 1. In addition, G_0 is the pre-exponential factor and ΔT is the

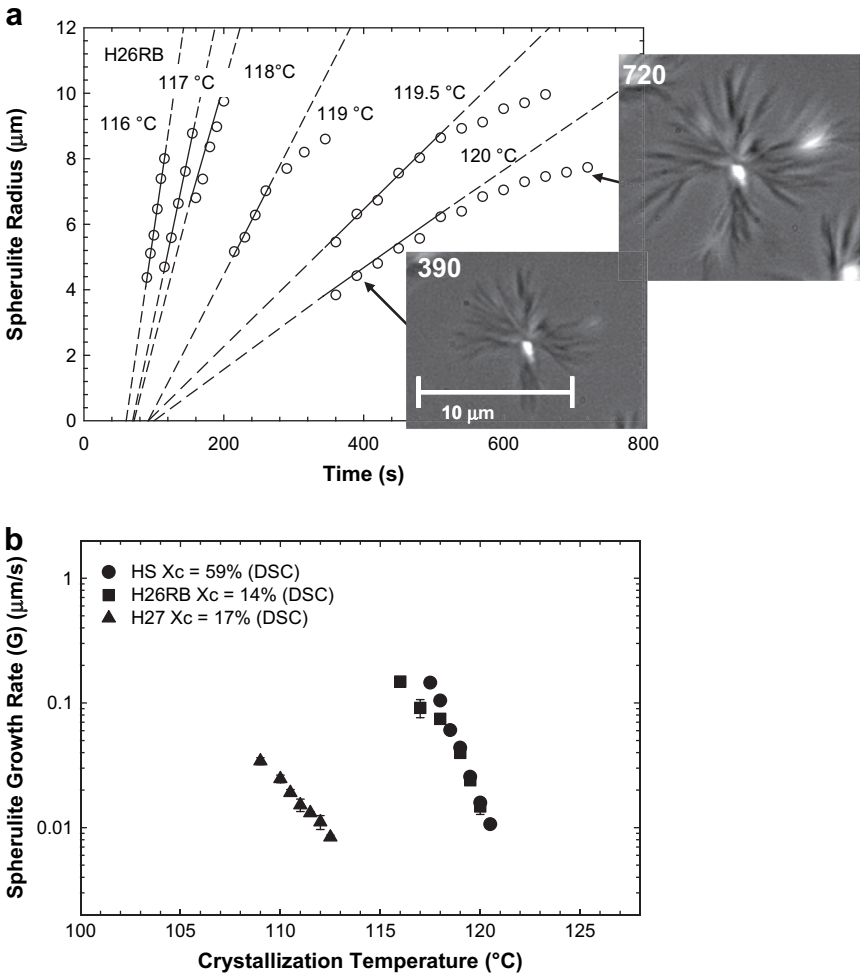

Fig. 7. Spherulite growth of the reactor blend H26RB: (a) spherulite growth as a function of time at various temperatures and (b) comparison of spherulite growth rate of HS, H26RB and H27.

undercooling $\Delta T = T_m^o - T_x$ where T_m^o is the equilibrium melting temperature. The nucleation constant K_g is defined as [28]

$$K_g = \frac{nb\sigma\sigma_e T_m^o}{\Delta H_f k} \tag{6}$$

where $n = 4$ for regimes I and III and $n = 2$ for regime II, b is the thickness of the crystal stem, σ is the lateral surface free energy, σ_e is the fold surface free energy, k is the Boltzmann constant, and ΔH_f is the heat of fusion of the polyethylene crystal. The equilibrium melting temperature T_m^o can be obtained from the relationship between melting temperature and lamellar thickness according to the simplified Thomson–Gibbs equation [29]

$$T_m = T_m^o\left(1 - \frac{2\sigma_e}{l\Delta H_f}\right) \tag{7}$$

where T_m is the melting temperature recorded by DSC and l is the lamellar thickness obtained by SAXS and the crystallinity from DSC.

The isothermally crystallized blocky copolymers exhibited a relatively broad SAXS diffraction ring corresponding to the long period. The ring shifted to progressively lower scattering angles as the soft block content increased. The corresponding Lorentz-corrected intensity curves provided the scattering vector at maximum intensity q_{max}, Fig. 8. The intensity curves also showed a slight decrease in q_{max} with increasing crystallization temperature. The long period L was calculated from q_{max} as

$$L = \frac{2\pi}{q_{max}} \tag{8}$$

and lamellar thickness l was taken as $l = LX_{vol}$ where the volume fraction X_{vol} was calculated from the weight fraction crystallinity X_c using the usual values of 1.000 g cm^{-3} for the crystalline density of polyethylene and 0.855 g cm^{-3} for the amorphous density of polyethylene [11]. The long period was also estimated from the AFM images of lamellar stacks. Although this method was considered qualitative, the agreement with SAXS was quite good, with the AFM estimates of L being 4–6 nm larger than the SAXS values.

The lamellar thickness is plotted according to Eq. (7) in Fig. 9. The data for each copolymer extrapolated to a common value of $T_m^o = 138$ °C. For comparison, reported values for T_m^o for HDPE vary from 138 to 144.5 °C [19]. According to

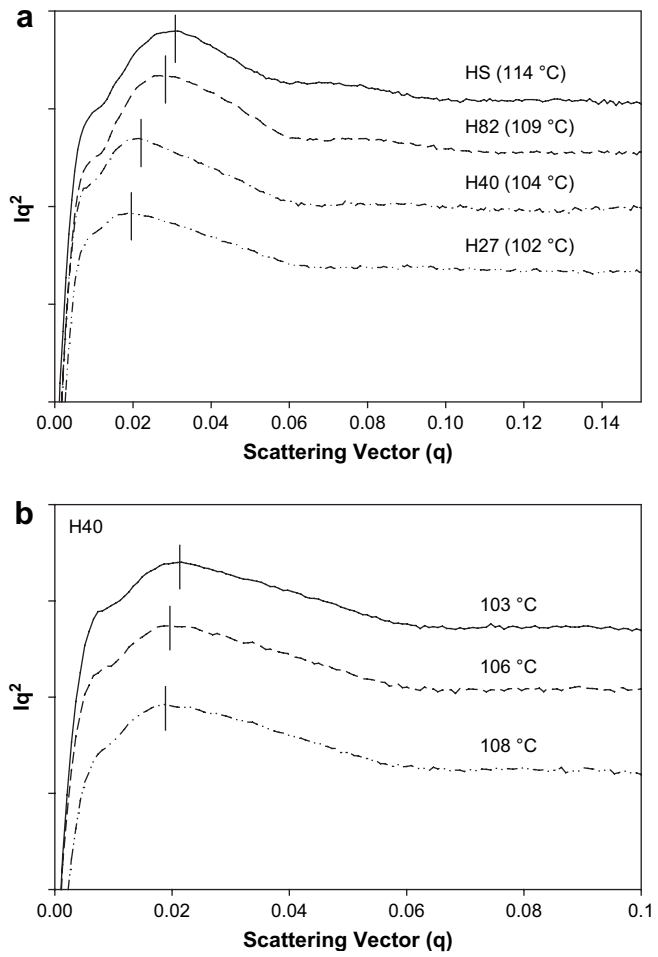

Fig. 8. Lorentz-corrected SAXS profiles: (a) HS and various blocky copolymers at the temperatures indicated and (b) H40 crystallized at different temperatures.

Eq. (7), the slope was expected to increase systematically with soft block content, and indeed this was observed for HS, H82 and H40. However, the result for H27 did not follow the trend.

To account for the discrepancy with H27, it was useful to examine the lamellar morphology of the isothermally crystallized polymers. Spherulites of H82 consisted of uniformly and densely packed, twisted lamellae, Fig. 10a. It was anticipated that the measured long spacing was representative of the entire volume and the bulk crystallinity was appropriate for determining the lamellar thickness. In contrast, stacked lamellae appeared in only some regions of the H27 spherulite, Fig. 10b. Lamellae in other regions were isolated or fragmented. The crystalline heterogeneity probably resulted from the distribution in block lengths and distribution in the number of blocks per chain. It can be imagined that chains with longer hard blocks and shorter soft blocks crystallized as stacks of long lamellae with the soft blocks excluded to

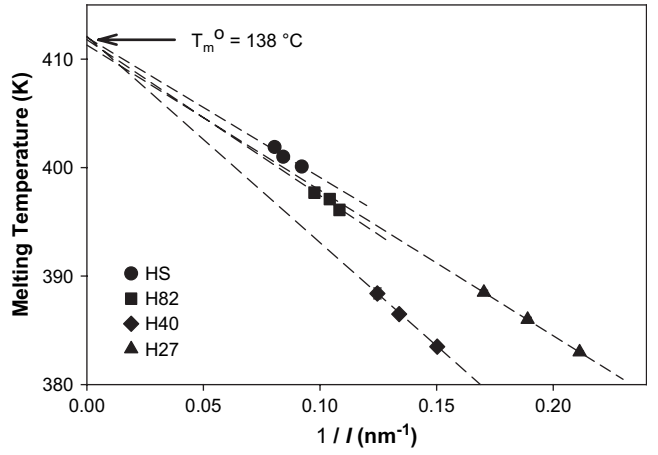

Fig. 9. Thomson–Gibbs plots for HS, H82, H40 and H27. The dashed line represents the best fit with extrapolations to $1/l = 0$ to determine T_m^o.

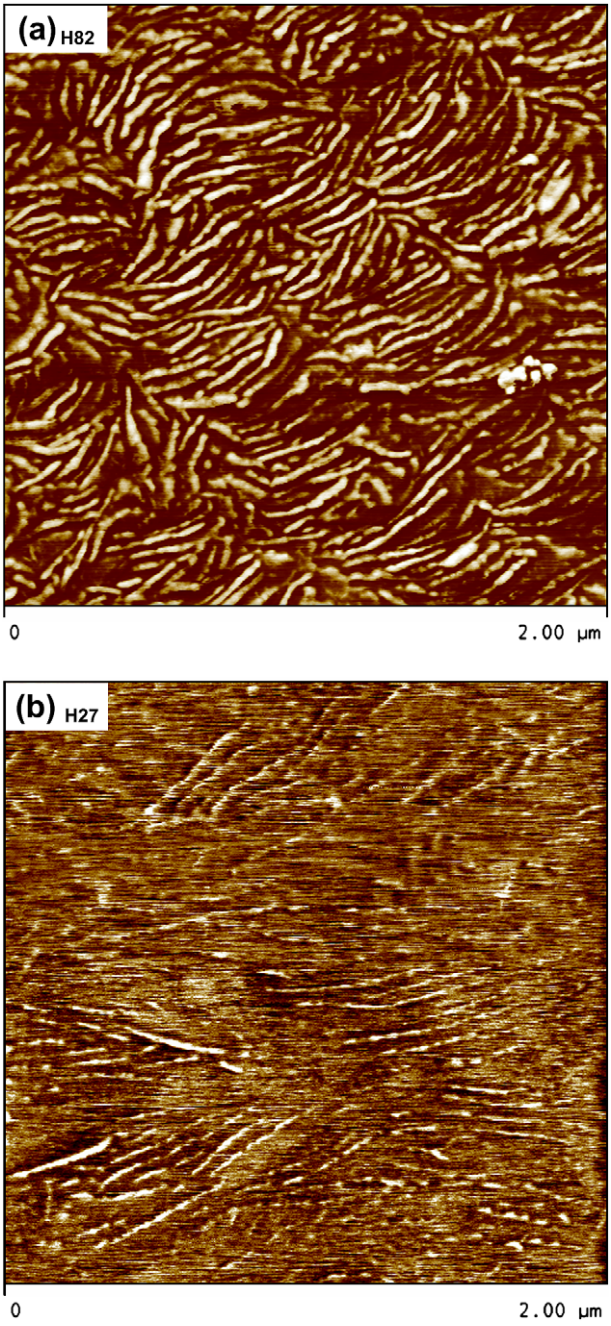

Fig. 10. High resolution AFM phase images showing the lamellar organization of (a) H82 and (b) H27.

the interlamellar regions. Conversely, the need to accommodate the large non-crystallizable blocks of chains with shorter hard blocks and longer soft blocks inhibited lateral growth of crystals and ordered stacking of lamellae. Locating non-crystalline blocks on the lateral edges of the crystals produced lamellae that appeared fragmented. In this situation, the SAXS preferentially sampled the lamellar stacks where the local crystallinity was higher than the average bulk crystallinity. The crystallinity of the lamellar stacks of H27 was estimated by measuring the lamellar thickness and lamellar separation in the AFM images. When the resulting value of 26 vol% was used to calculate lamellar thickness, the data for H27 shifted to the left-hand side of the line for H40 with a higher slope and without changing the T_m^o intercept.

The spherulite growth rate is plotted in Fig. 11 according to Eq. (5) with $U^* = 5736$ cal mol^{-1} [30], and displayed an excellent fit. Linear plots were obtained in all cases with slope K_g that gradually increased with increasing soft block content. In this case, a bulk quantity, i.e. the spherulite growth rate, was used in the calculation and the data for H27 followed the trend established with the higher crystallinity copolymers. The crystallization temperatures used in the study fell into regime II crystallization [19]. The surface free energy σ_e was calculated from Eq. (6) taking $n = 2$, $b = 4.15 \times 10^{-8}$ cm, $\sigma = 11.8$ erg cm^{-2} and $\Delta H_f = 2.8 \times 10^9$ erg cm^{-3} [30]. The values obtained for σ_e are included in Table 1. The value of 111 erg cm^{-2} for HS was slightly higher than the reported value of 100 erg cm^{-2} for polyethylene due to the increased disorder of the fold surface brought about by 0.5 mol% comonomer [19]. Statistical distribution of comonomer was very effective in disrupting the fold surface regularity as demonstrated by a σ_e of 204 erg cm^{-2} for EO2.8.

The presence of soft block that was not covalently linked to hard block (H26RB) had almost no effect on σ_e. Covalently linking hard blocks to soft blocks increased σ_e to some extent. As the amount of non-crystallizable soft block increased, σ_e increased from 111 erg cm^{-2} for HS to a maximum of 143 erg cm^{-2} for H27, Table 1. However, compared to the effect of even a small level of statistical branching, the effect of soft blocks on fold surface order was quite modest.

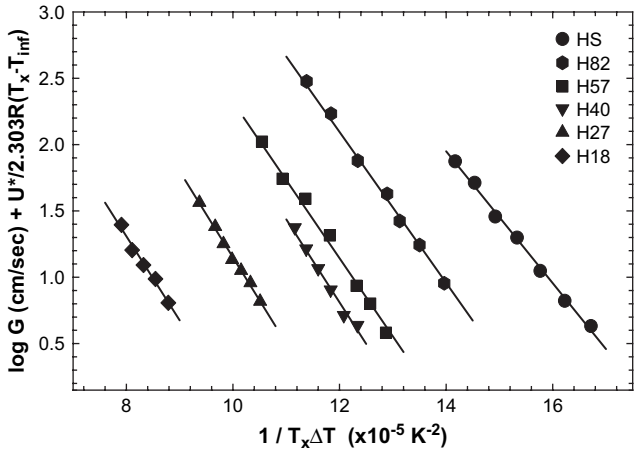

Fig. 11. Lauritzen–Hoffman plots of the spherulite growth rate of HS and the blocky copolymers. The solid line represents the best fit; the slope was used to calculate σ_e.

4. Conclusions

Isothermal crystallization kinetics of blocky ethylene–octene copolymers synthesized by chain-shuttling polymerization was studied as a function of the crystallizable hard block content. The rate of bulk crystallization from the homogeneous melt slowed somewhat as the amount of hard block decreased from 100 to 18 wt%. However, due to the blocky architecture, crystallization was rapid even in copolymers with a relatively large fraction of non-crystallizable soft block. The bulk kinetics conformed to the Avrami analysis with exponent of 3, which was consistent with spherulitic growth with athermal nucleation. Crystallization of all the copolymers as space-filling spherulites made it possible to measure the spherulite growth rate. The linear growth rate exhibited the same dependence on soft block content as the bulk crystallization rate. The fold surface energy was extracted from an analysis of the growth rate according to the Lauritzen–Hoffman theory. A gradual increase in the fold surface energy with soft block content reflected the increasing disorder of the fold surface.

Two comparisons examined the impact of the blocky architecture. Comparison with a statistical copolymer revealed that the total crystallinity was determined primarily by the total octene content regardless of chain architecture, whereas the crystallization habit and crystallization kinetics were strongly affected. Only a few percent of a statistically distributed comonomer dramatically reduced the crystallization rate. Due to the reduction in spherulite growth rate compared to the nucleation rate, statistical copolymers formed spherulites only if the comonomer content was quite low. The very high fold surface energy revealed the large disruption in fold surface regularity that was brought about by exclusion of comonomer units. A second comparison was made with a miscible blend of hard block polymer and soft block polymer that was obtained by omitting the chain-shuttling agent from the polymerization. In the absence of covalent linkages, the soft block polymer readily segregated into the interlamellar and interspherulitic regions during crystallization. As a consequence, the blend rapidly crystallized as ‘‘open-arm’’ spherulites.

Acknowledgments

The authors thank Ben Poon of The Dow Chemical Company for technical assistance and material characterization. This research was generously supported by The Dow Chemical Company.

Appendix. Supplementary data

Supplementary data associated with this article can be found, in the online version, at doi:10.1016/j.polymer.2007.12.046.

References

[1] Arriola DJ, Carnahan EM, Hustad PD, Kuhlman RL, Wenzel TT. Science 2006;312:714.
[2] Wang HP, Khariwala DU, Cheung W, Chum SP, Hiltner A, Baer E. Macromolecules 2007;40:2852.
[3] Minick J, Moet A, Hiltner A, Baer E, Chum SP. J Appl Polym Sci 1995;58:1371.
[4] Hamley IW, Castelletto V. Prog Polym Sci 2004;29:909.
[5] Mohajer Y, Wilkes GL, Wang IC, McGrath JE. Polymer 1982;23:1523.
[6] Quiram DJ, Register RA, Marchand GR, Ryan AJ. Macromolecules 1997;30:8338.
[7] Rangarajan P, Register RA, Fetters LJ. Macromolecules 1993;26:4640.
[8] Okamoto S, Yamamoto K, Nomura K, Hara S, Isamu A, Sakurai K, et al. J Macromol Sci Part B Phys 2004;43:279.
[9] Sehanobish K, Patel RM, Croft BA, Chum SP, Kao CI. J Appl Polym Sci 1994;51:887.
[10] Bensason S, Minick J, Moet A, Chum S, Hiltner A, Baer E. J Polym Sci Part B Polym Phys 1996;34:1301.
[11] Brandrup J, Immergut EH. Polymer handbook. 3rd ed. New York: Wiley; 1989. SectV/17.
[12] Hu YS, Rogunova M, Schiraldi DA, Hiltner A, Baer E. J Appl Polym Sci 2002;86:98.
[13] Stachurski ZH, Macnicol J. Polymer 1998;39:5717.
[14] See Table 2 in Supplementary data.
[15] Bassett DC. Principles of polymer morphology. Cambridge University Press; 1981. p. 146.
[16] Piorkowska E, Galeski A, Haudin JM. Prog Polym Sci 2006;31:549.
[17] Wunderlich B. Macromolecular physics, vol. 2. Academic Press; 1976. p. 115.
[18] Sasaki S, Sakaki Y, Takahara A, Kajiyama T. Polymer 2002;43:3441.
[19] Lambert WS, Phillips PJ. Macromolecules 1994;27:3537.
[20] Hoffman JD, Frolen LJ, Roadd GS, Lauritzen JI. J Res Natl Bur Stand Sect A 1975;79:671.
[21] See Table 3 in Supplementary data.
[22] Sharples A. Introduction to polymer crystallization. St. Martin's Press; 1966. p. 44.
[23] Di Lorenzo ML. Prog Polym Sci 2003;28:663.
[24] Keith HD, Padden FJ. J Appl Phys 1964;35:1270.
[25] Lee CH. Polymer 1998;39:5197.
[26] Okada T, Saito H, Inoue T. Macromolecules 1990;23:3865.
[27] Keith HD, Padden FJ. J Appl Phys 1964;35:1286.
[28] Lauritzen JI, Hoffman JD. J Res Natl Bur Stand Sect A 1960;64:73.
[29] Wunderlich B. Macromolecular physics, vol. 3. Academic Press; 1976. p. 1.
[30] Hoffman JD, Miller RL. Polymer 1997;38:3151.